Thermographic Inspection System for Surface Coating Defects on Aircraft Fuselage

WPMY Thilakarathna[1#], AA Ziyard[1], ND Wijesinha[1] , KVP Dhammika[2] and GMSM Gaspe[1]

[1]*Department of Mechanical Engineering, Faculty of Engineering, KDU*

[2]*Department of Electrical, Electronic and Telecommunication Engineering, Faculty of Engineering, KDU*

[#]thilakarathnamy@kdu.ac.lk

Abstract : The aircraft *outer shell is coated with a corrosion-resistant layer because its alloy does not possess sufficient intrinsic resistance to wear and corrosion. Impacts by small particles or large objects such as bird strikes can lead to damage to the coated surface inducing surface defects. Micro cracks initiated due to surface damages create stress concentration zones which could lead to catastrophic failure of the aircraft due to fatigue crack formation. Therefore, the importance of regular inspection of surface coating is highlighted. Visual inspection is widely used for surface damage identification but, manual procedures with the bare eye are time-consuming and lead to human errors. Effective automation of the inspection can be considered a viable solution. The aim of this project was to develop an automated inspection system based on non-contact, non-destructive Infrared Thermography to identify defects on an aircraft's surface coating. The system developed was a two-axis gantry attached to a four-wheel structure equipped with a tiltable thermal camera assembly and a control panel. The inspection method follows the sequence; Firstly, thermal image capturing. Next, image processing and identifying the defect area. Thirdly, giving a signal to the operator if a defect is present. The system was tested on a significant dataset and its capability of detecting surface defects on an aircraft's coating was demonstrated. The results suggest an automated thermographic inspection system for surface coating defects on aircraft fuselage can successfully replace visual inspection leading to a 9.25 % increase in efficiency and minimizing its inherent disadvantages.*

Keywords*: Thermographic Inspection, Aircraft Defect Detection, Image Processing*

1. Introduction

The outer coating of an aircraft is expected to have a prolonged life whilst enduring extreme conditions to ensure the integrity of the aircraft structure. Wear/damage of the coatings due to the impact of bird strikes initiate surface defects which can induce serious structural failure with time. Thus, the detection of coating defects became a prime importance in aeronautical applications and it's understood that regular inspections on coatings must be carried out through in-service monitoring to ensure satisfactory lifespan of aircraft surface structure (Sause, 2021).

In the field of engineering, Non-Destructive Testing (NDT) is the most common technology that used to detect and evaluate flaws in materials: cracks, defects or variations in structural properties of materials. Traditional NDT methods involve visual inspections, radiography, ultrasonic testing (UT), magnetic particle testing, penetration testing, eddy current testing etc (Dwivedi, Vishwakarma

and Soni, 2018). Out of which, visual inspection is the most popular method that used to identify abnormalities in aircraft structure, but it creates greater maintenance downtimes and human errors(Stamm et al., 2021). Especially, it is not applicable for complex and sensitive aircraft structural inspections like identifying coating defetcs.

Infrared Thermography (IRT) is a popular solution which has emerged in recent years to address complex NDT problems in aviation industry. However, in the conventional method of thermographic inspection also involves the operator continuously monitoring the aircraft surface manually, through a view finder of the thermal imaging equipment to identify the abnormalities produced in the thermal image. In this manual thermographic inspection method, the operator requires sufficient expertise and is under continuous pressure to accurately identify and take the required action of confirming a surface defect(Srajbr, Bräutigam and Dillenz, 2012).

The aim of this project is to elaborate an innovative method for identification of aircraft coating defects based on Infrared Thermography whilst reducing the burdens of visual inspection method. This paper describes designing, fabricating and testing a scaled down automated system which can identify surface defects on an aircraft's fuselage coatings using non-contact, non-destructive Infrared Thermographic inspection.

2. State of the Art

In the Aerospace industry, NDT techniques are used to detect the presence of abnormalities in aircraft structures. Review of NDT methods for composite materials by Gholizadeh (2016) provides an overview of basic types of NDT methods that are used in the Aerospace (Aero) Industry: Visual Inspection, UT, Radiography, IRT, Vibration Methods, Shearography and XCT. Out of which Infrared thermography is a revolutionary method that used to analyse flaws in materials in the Aero industry. IRT refers to a non-contact NDT method where thermal information obtained from a specimen is analyzed and produced an image of temperature variation of the specimen as output.

Some literatures explicitly discusses the use of IRT in Aero Industry. Yang et al (2019) has presented an IRT based Crack Detection method of steel sheets using Convolutional Neural Networks (CNN). Shang et al (2007) developed a climbing robot with a scanning arm to detect loose rivets in aircraft fuselage through thermal imaging. Another IRT application was In-plane heatwave thermography inspection technique for fasteners in aircraft fuselage by Stamm et al (2021). Cramer and Winfree (2006) from NASA studied the application of IRT inspection techniques to the space shuttle thermal protection system. Accordingly, there were various NDT techniques that have been used by NASA in the examination of the Reinforced Carbon-Carbon (RCC) panels in space shuttles, but they found thermography is the most effective inspection alternative to other methods. NASA is currently using the commercial infrared thermography system called EchoTherm for RCC Inspections.

Eddazi and Belattar (2018) have proposed a method to evaluate Aircraft Fuselage corrosion resulted from chemical reactions by using IRT and Finite Element Method. In that work, simulations were based on changes in heat flux and thickness of corrosion that determine the degree of detectability of the IRT method with the analysis of resulted temperature differences. Srajbr, Bräutigam and Dillenz (2012) proposed an induction excited thermography for fatigue crack detection in the aluminum skin of the Boeing 737. In their project, eddy current testing was intended to be replaced by an automated thermographic sensor positioned on a robot which offers non-conact extensive testing of structures by a defect selective visualization of induction heating irregularities.

However, according to the journal article Damage Detection Systems for Aerospace by Sause (2021), it's important to understand the defect types in order to implement defect detection systems to produce the desired structural integrity. Thus, basic types of aircraft structural material include metals, composites, coatings, and adhesively bonded and welded joints. Out of which coatings (thin or thick film) in aircraft surface is there to reduce the effect of corrosion/wear that can cause serious safety effects. According to the journal article of Structural Defect Types by Faisal et al (2021), wear/damage of the coated surface due to the impact of small sand particles or large objects such as bird strikes and indentations of the structure during the handling process are the most common reasons of inducing surface defects. That article emphasizes the importance of preventive and remedial inspection methods on aircraft surface coatings to rectify any unexpected defects.

Although the most common NDT method of identifying surface defects is visual inspection, Stamm et al (2021) states that the manual visual inspection performed with the naked eye has inevitable drawbacks whereas its outcome is subjective to individual inspector and time consuming. A review on NDT by Dwivedi, Vishwakarma and Soni (2018) reveals that visual inspection is not suitable to detect small flaws on surfaces like coating scratches which were mentioned above.

The proposed automated thermographic inspection system for aircraft fuselage coating defects detection aims to fulfill the drawbacks in visual inspection by replacing it with Infrared Thermography.

3. Methodology

Based on the identified research gap, a methodology for developing the thermographic inspection system was formulated. The proposed system was a rover with a double-axis gantry attachment for scanning the aircraft in an aircraft hangar. Three major parts of the system were (1) the Driving Trolley, (2) the Camera Lifting and Tilting Mechanism and (3) the Controlling Mechanism. The reference aircraft for the inspection system design was the PT-06 Aircraft accessed through the Air Support Wing (ASW) - Ratmalana, Sri Lanka.

A. Conceptual Design

Concept generation of the project involved the integration of a design table (Table 1) with a concise rating table based on fragmented 7 sub parts of the main system: (1) Thermal Camera (2) Lifting Mechanism (3) Lifting actuators (4) Controller for Thermal Imaging and Processing (5) Camera Tilting Mechanism (6) Power source (7) Defect Detection Indicator. The Design Table was based on the extensive Literature Review done under the aforementioned categorization.

The range of applicable technologies for each part was identified and integrated to form 4 design concepts. The selected sub-parts were individually analyzed based on their unique advantages and disadvantages by giving scores according to specific weighted design attributes : (1) Thermal Camera – Resolution, Field of View (2) Lifting Mechanism – Stability (3) Lifting Actuators – Torque applicability, complexity (4) Controller for Image Processing – Processing Capability, Availability (5) Camera Tilting Mechanism – Area Coverage , Weight (6) Power source – Energi Density, Weight (8) Defect Detection Indicator – Visibility , Understandability. Cost was primary selection attribute for all the sub parts. Completed rating table opened a path for determining the quantitative best design using total weighted score and the selected design was Design 2 which had the total weighted score of 77.75.

Table 1. Design Table

Sub Parts	Design 1	Design 2	Design 3	Design 4
Thermal Camera	FLIR A35	FLIR Lepton 3	Adafruit	FLUKE flexcam
Lifting Mechanism	Crane	Linear Drive	Linear Drive	Hydraulic Scissor lift
Lifting actuators	Hydraulic Piston	Electric Motor	Electric Motor	Hydraulic Piston
Controller for Imaging Processing	Intelligent Global Controller	Raspi	Arduino MEGA 2560	PC
Camera Tilting Mechanism	Platform Pan/Tilt	Pan and Tilt	Solid Mount	Motor on Motor Mount
Power Source	Lithium Battery	Tether	Lithium Battery	Lead Acid Battery
Defect Detection Indicator	Display	Display, LEDs, alarm	Alarm	Display

B. Design Considerations

1) Rover and Lifting Mechanism: A Trolley with wheels was selected for the rover. Trolley proportions were based on the PT6 aircraft used for testing, total area coverage for one static placement of the system and total weight of mounting components.The respective calculations were done accordingly.

To capture the thermal images of the focus area, the lifting mechanism was needed to be embedded in the system which can mount and carry the camera for scanning the surface. Two-axis gantry consist with two linear drives was the selected method for the lifting mechanism. One unit of linear drive consists of a ball screw, guide rails, linear bearings, end mounts and guide mount. Based on pre-load dynamic torque calculations, selected two linear drives were ball screw SFU 1605 and SFU 1204. As shown in Figure 1, a linear static stress analysis was carried out using SOLIDWORKS Simulation software by applying relavent stiffness data in order to confirm the rigidity of the selected vertical ball screw SFU 1605.

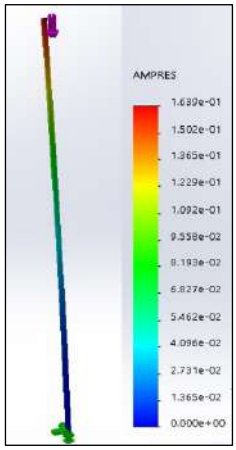

Figure 1. Stress Analysis Diagram for Vertical Ball Screw

Two linear drives were decided to be driven by stepper motors and to estimate the power requirements for both forward and backward movements, respective calculations were done by using torque requirements based on dynamic loading conditions. For Horizontal ball screw drive torque and back drive torque, calculations were done by equation (1) and for vertical linear drive it was done by equation (2).

$$T\_h = (S\_L\ P\mu)/(2\pi E\_ff\ ) \quad (1)$$

where : P = Applied Dynamic Load (N)

S_L= Lead of Screw (m)

μ = Coefficient of sliding friction

Eff = Ball screw efficiency (90%)

$T\_v = (J + (mr\text{^}2)/e\ ) \times a/r\ +\ r/e \times mg$

(2)

where : m = Mass of the load and the nut

J = Moment of inertia

a = Upward acceleration

r = Transmission ratio of lead

screw (5mm/rev)

e = Fractional efficiency of Lead Screw (90%)

T_h (forward) = 0.001Nm

T_h (backward) = 0.00015Nm

T_v (forward) = 3.1Nm

T_v (backward) = 0.031Nm

Nema 23 and Nema 17 stepper motors were selected based on above calculated drive torque requirements and the respective power requirements were 16.88W and 7.8 mW.

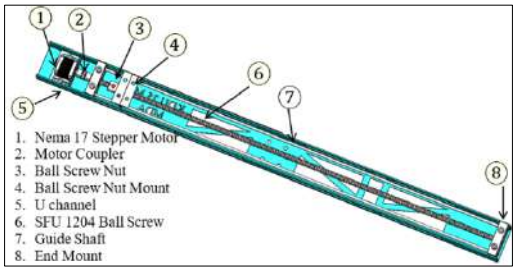

Figure 2. Design of Horizontal Linear Drive

2)Thermal Camera and Tilting Mechanism: Based on the extensive comparison done in the design table FLIR Lepton Thermal camera was identified as the most economical and accurate thermal camera for this application. From lepton series, FLIR Lepton 3 was selected as per the required specifications of compact size, resolution of 160 (h) x 120 (v) active pixels and shutter capability for image capturing. Since the camera setup was needed to be attached to the horizontal ball screw nut, a camera mount was designed for Lepton 3 camera. To capture the thermal image effectively, the camera must be turned to face the aircraft surface with optimal depth of field (DOF) which is 30 cm. Thus, a servo-controlled tilt mechanism was designed with IR sensor which can detect the ideal DOF.

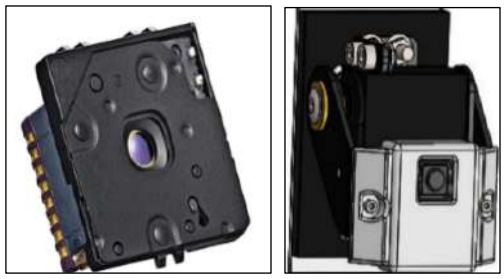

(a) (b)

Figure 3. (a) FLIR Lepton 3 Thermal Camera (b) Tilting Mechanism Design

In designing stage, all the mechanical components: Trolley, Lifting Mechanism, Camera Setup and Tilting Mechanism were drawn part-wise using SolidWorks software. Respective components were assembled to get the visual representation of the final system given in the Figure 4.

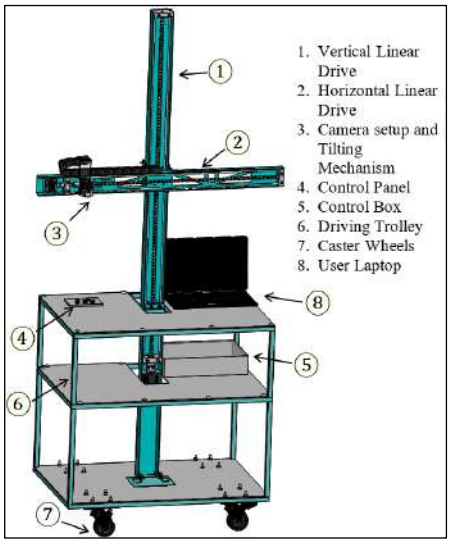

Figure 4. Final Design of the Mechanical Systems

C. Fabrication

Fabrication of the project was fragmented into 3 sub-assemblies: Trolley, Lifting mechanism with horizontal and vetical linear drives, Tilting mechanism with Camera setup. Starting

with trolley fabrication, skeleton of the trolley was fabricated using 19 x 19 x 1.4 mm steel box bars welded together. Plywood planks were fixed to the skeleton as shelves with plastic toggles using 6mm drilled holes. To drive the trolley, pair of locked caster wheels and universal cater wheels were used.

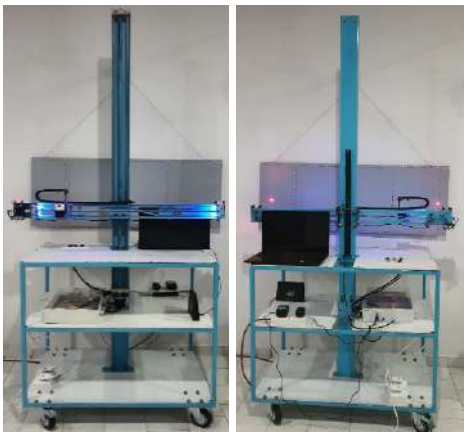

Figure 5. Finalized System

Next, fabrication of the lifting mechanism was initiated part by part. For one linear drive, there were 8 parts as shown in Figure 2. According to the dimensional requirement, ball screw was needed to be modified by using lathe machine and end mounts made out of Teflon were lathed and drilled to place bearings and guide rails. For motor mounts and the ball screw nut mount, 5 mm steel metal sheets were laser cut and bent in 90 degrees with metal bending machine. The whole linear drive setup was mounted on an U channel made out of 2 mm thick steel metal sheet and the guide rails were 6 mm and 8 mm stainless steel rods. Finally, the fabricated components of lifting mechanism together with camera setup were assembled to the trolley for the completion of the inspection system (Figure 5).

D. Image Processing

1) Configuration of Thermal Camera and Controller: The microcontroller for image processing was selected under 4 main factors: power and storage capacity, compatibility with thermal camera and reliability. Thus, Raspberry Pi 4 model B (Raspi) was selected as the suitable controller for image capturing and processing system. The circuitry was integrated with Lepton 3 Thermal Camera, PureThermal 2 I/O board, Raspi and 5V 3A power supply as shown in Figure 6. VNC Viewer was used as the method of accessing the Raspi remotely. Configuration of Raspi was done to operate the thermal camera Lepton 3 for testing the thermal images captured, verifying the applicability of it.

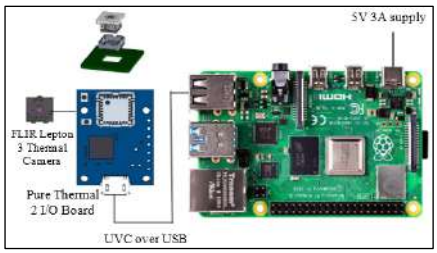

Figure 6. Connection Diagram of Image Capturing System

There were two viewing softwares of using the Lepton 3 interfaced to a Pure-Thermal 2 I/O board on a Raspi called GetThermal and Parabilis thermal. Although the GetThermal software was the Purethermal 2 proprietary software its dependency on OpenGL driver presumably brought upon indistinguishable errors when executing GetThermal. Therefore, Parabilis thermal was used since the functionality was same even though proprietary software was not used. Parabilis thermal can only allow recording of a video of the thermal view in HDF5 format but the proposed system requires image capturing as the project aims to fully automate the process of defect detection. Therefore, Parabilis Thermal was used to create the dataset of 'defect' and 'no defect' images by recording a video and later isolation of individual frames were done through the post processing script of Parabilis Thermal.

Before initiating the image capturing, required calculations were done to find the field of view of an image captured by thermal camera using specifications of the Lepton 3. Thus, with 30

cm ideal DOF, horizontal and vertical field of views were 31. 9 cm and 28.5 cm respectively.

2) Thermal Imaging and Image Processing: Lepton 3 camera was used to capture 70 thermal images containing 44 images of defects and 26 images with no defects by using a fuselage panel removed from an aircraft of Sri Lankan Airforce. The conditions were simulated based upon operating the equipment on an aircraft immediately after landing whilst maintaining the surface temperature of the aircraft above 36˚C. To obtain the required heat of 39˚C test piece was heated by a heat gun. The defects were simulated by impacting the test piece using a sharp metal rod to demonstrate a bird strike on the aircraft. To capture the videos in HDF5 format, RecordIR script of Parabilis Thermal software was used and PostProcessIR script was used to separate frames in the video to be saved as images in PNG format.

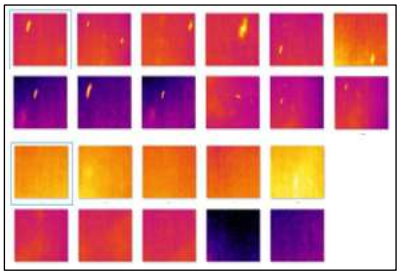

Figure 7. Part of source dataset of thermal images

70 images were flipped and mirrored to make a dataset of 560 8-bit images (Figure 7) and those RGB images were converted to gray scale (Figure 8) by using python script to perform the image manipulations using the Pillow library.

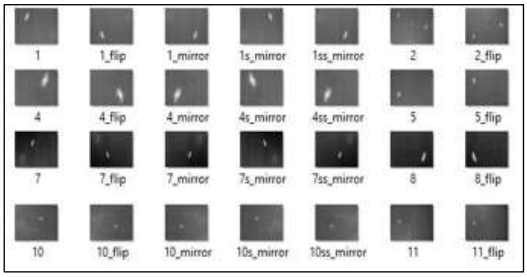

Figure 8. Part of dataset after manipulation and gray scaling

Since the thresholding was selected as the segmentation method for this system, the cv2.threshold() function within the OpenCV library was used to perform thresholding on the images. Thresholding involves analyzing the image at the pixel level to separate background from foreground. As thresholding binarizes an image, the grayscale image was converted to a binary image making the pixels either 0 or the maximum i.e 255 (maxval). The gray scaled thermal image can be defined as a function f (x, y) whereas the threshold image g (x, y) can be defined as follows:

T= Adequate Threshold value

$$g(x,y) = \{\blacksquare(maxval \quad if\ f(x,y) \geq T@\ 0 \quad otherwise)\dashv$$

Two thresholding methods based on grayscale histograms were considered – Otsu's method and Triangle method. Otsu's method computes an optimum value for '**T**' assuming that the image consists of two classes, the background and the foreground represented by a bimodal grayscale histogram. It computes a global threshold by minimizing the weighted variance between the two classes. In the triangle method a line is constructed between the peak and the far-end of the histogram. The threshold is the greatest distance (dmax) between the line and the histogram. Triangle method was selected as it clearly isolated the defect than Otsu's method which produce more images with noise causing incomplete separation of the defect area. Figure 9 shows the histogram that resulted from defective image after triangle thresholding and the basis for calculating the threshold value.

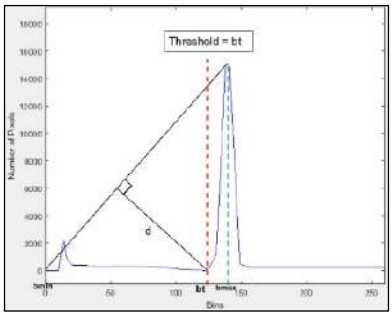

Figure 9. Histogram resulted from Triangle Thresholding

For filtering, 5 most frequently used image filters in image pre-processing: Mean, Gaussian, Median, Conservative and Image Arithmetic filers were explored. As per the comparison, it was observed that the Mean, Gaussian, Median and Conservative filters tend to merge both defect areas and non-defect areas. From the Image Arithmetic matrix addition or subtraction the brightness and contrast of the image was manipulated. Subtraction arithmetic filter was chosen to be used as it reduces the brightness, resulting in defects with higher pixel intensities being distinguished. It was applied before the thresholding function because when triangle thresholding is applied, the defect area will be unclear since the contrastive strength of the image is low.

Final script was formulated incorporating grayscale conversion, subtraction arithmetic filtering, triangle thresholding and an if conditional active pixel counting to obtain a defect judgement regarding an image that is captured by the thermal camera. Respective sequence of defect identification process is mentioned in Figure 12.

E. Control System

Control system had 2 subsystems which were controlled by two different controllers: Raspberry Pi to control the image capturing and processing, Arduino MEGA 2560 for controlling lifting and tilting mechanism (Figure 10). Operation of image processing system controlled by Raspi was according to the explanation given in the previous section.

Controller 2: Arduino Mega was for controlling lifting and tilting mechanism. Since the lifting mechanism was with two ball screws driven by stepper motors Nema 17 and 23, the respective coding was needed to be done after setting the circuitry. Circuitry of one linear drive was with set of components: Stepper motor and driver, SMPS controlled by Arduino.

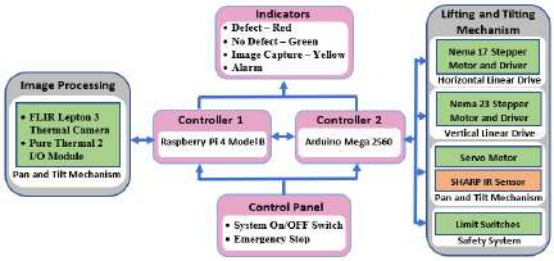

Figure 10. Structure of the Control System

Prior to commence the programming of lifting mechanism controlling section, step count calculations of stepper motor were done correlating with the camera's field of view (FOV). Based on the calculations, FOV of Lepton 3 was 31.9 x 28.5 cm when camera is placed 30 cm (DOF) perpendicular to the capturing surface. Stepper motor coupled with horizontal linear drive was to stop in each 29.5 cm linear movement to capture images as horizontal field of view (HFOV) is 31 cm. Thus, vertical linear drive stops at every 26 cm (VFOV) distance movement. With those decided values, the step count per run was calculated and programming for combination of two linear drives was conducted. In this system the total area coverage per run was 135 x 120 cm^2 and it was divided to 20 squares of 31 x 26 cm which covers per take when the camera is set up 30 cm distance perpendicular to the test surface. Figure 11 shows the area coverage and the graphical view of lifting mechanism moving algorithm.

Camera Pan/tilt mechanism with servo motor MG955 attached to the horizontal linear drive was also controlled by Arduino. According to the controlling algorithm when the horizontal linear drive stopped to take the image, servo motor rotated and IR sensor attached to it was

used to identify the ideal perpendicular distance (30 cm) with curvy aircraft surface before image capturing.

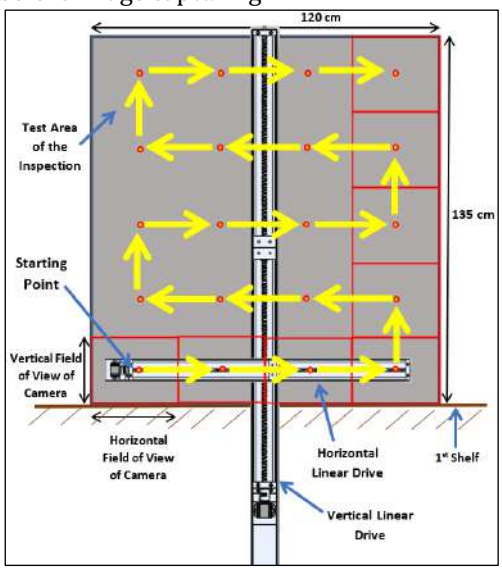

Figure 11. Area coverage and graphical view of lifting mechanism movement

Explaining the overall algorithm of the control system, after accurate positioning of the equipment using laser beams, to start the operation of the testing equipment "Start" button was there to press and then start signal is read by the Raspi, communicating it to the Arduino by using Serial Communication. With the continuous start signal given from Raspi, Arduino take action on the operation of lifting and pan/tilt mechanism by initiating the servo motor for the tilt setup and the stepper motors for linear drives appropriately according to specified functions in code. When the specified number of steps has reached in the horizontal operation stepper motor, a delay will be initiated on further movements of the camera whilst the Arduino sends a signal to the Raspi to initiate the camera capture python script and it's indicated by yellow LED. After the camera capture script is initiated, the image is processed and judged for defects. If there is no defect, the Raspi sends a serial command to the Arduino as "No Defect" and if condition continues the Arduino operation appropriately for the "No Defect" command. Simultaneously, the Raspi lights a green LED to indicate the operator of no defect. However, if it's determined that there is a defect, then the Raspi send the serial command "Defect" and it's indicated by red LED and alarm. This process (Figure 12) follows on a loop till the end of the total test area leading to the re-positioning of the equipment by the operator and continuing the process.

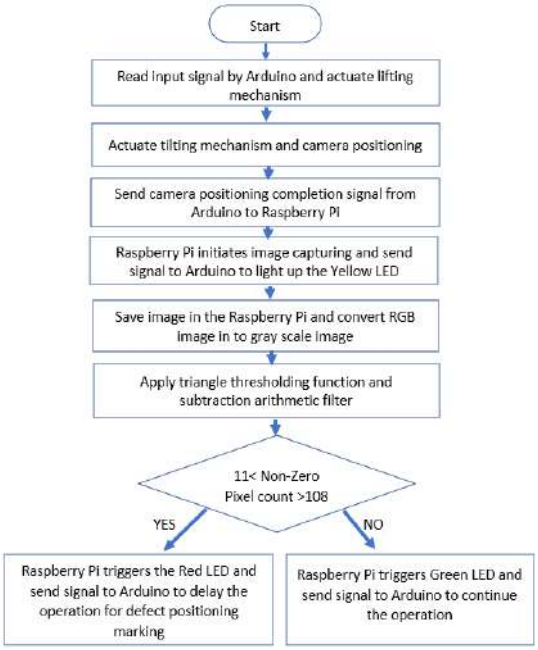

Figure 12. Control Flow

4. Results and Discussion

The main aim of this project was to develop a prototype of an automated system that can test for surface coating defects on a aircraft fuselage using non-contact, non-destructive IRT inspection and relieve the uncertainty in manual inspections. During the project completion, equipment was segmented by its main components and segment vise testing was done after fabrication prior to finalizing the system.

Especially considering the image processing system, different conditions that the thermal camera would possibly encounter such as low light, high exposure, shadow on surface and abstract angle conditions was explored whilst testing. A stock camera image with defect was

analyzed using same conditions to justify the use of the thermal camera instead of a normal camera for the equipment.

As aforementioned, during image processing stage, two types of threshold segmentation methods were compared to confirm the system applicability. It was observed that the Triangle method was better than the Otsu's method in dealing with effectively defining the foreground to the defect area since it brought less amount of noise to the foreground. Following results shows the comparison of two thresholding methods and noise apperance.

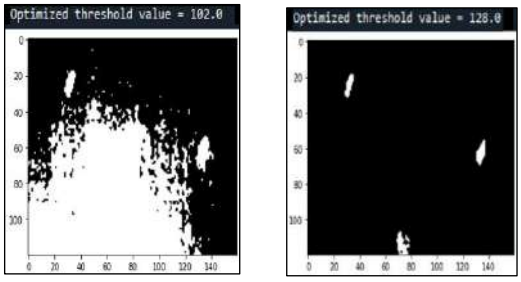

(a) (b)

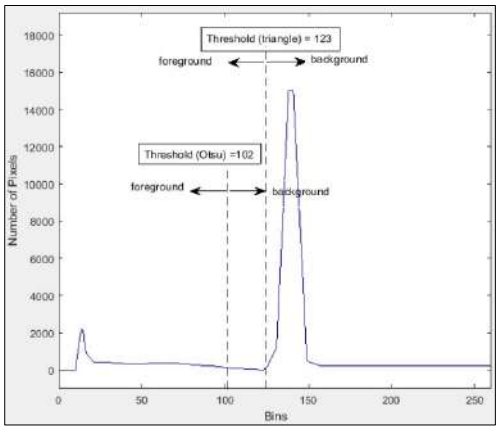

Figure 13. (a) Otsu's thresholding method (b) Trianlge thresholding method (c) Comparison of Otsu's method vs Triangle Method

As per the results, for the selected defective image threshsolding values for Otsu and Triangle method were 102 and 128 respectively (Figure 12). Respective histogram clearly emphasize the separation of background and foreground.

According to the results obtained after analyzing all the source data set underwent triangle thresholding it was determined that the pixel count range of defect images is between 11 to 108 non-zero pixels (Figure 13). Results inferred that a defect will be present for images with non-zero pixel counts above 11 and below 108. Further research is to be done for the integration of machine learning algorithm to create a self-learning system that can identify the region of non-zero pixel range.

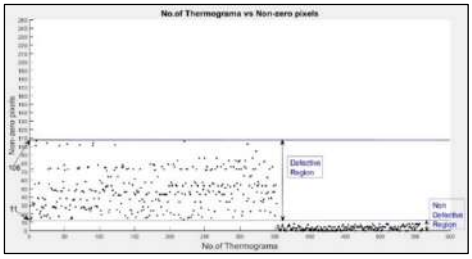

Figure 14. No.of Thermograma vs Non-zero pixels

For this inspection system, the total area coverage per one static placement of the system was 16,200 cm^2 and the total time taken for the inspection procedure for one static placement of the system was 18 mins and 55 secs whereas the manual inspection took 20 mins and 40 secs increasing the overall efficiency by 9.25%. Hence, the estimated inspection time for the total area coverage of PT 6 aircraft is 5 hrs and 42 mins. Further research is required to analyze the applicability of this system for surface defect inspections of large-scale aircraft.

5. Conclusion

The prototype of a thermographic inspection system for surface defects on aircraft was developed to introduce a novel concept to surface coating defect detection and to overcome the drawbacks of the existing manual inspection methods. As identified in the methodology, the worker involvement and the total time required for manual inspection were reduced by automating the camera lifting and tilting mechanism and due to the

embedded image processing system with an automated defect indication mechanism. Research continued improving the image processing system with a machine learning algorithm and further research needs to be done to improve the system design, with an automated navigation system and IOT-based indication system, to obtain zero worker involvement in the inspection procedure. As the experimental results confirmed the functionality of the prototype, it can be concluded that the Thermographic Inspection System for surface defects on aircraft is ready for further research in commercializing the equipment, building its accuracy, and showcasing it to the world.

References

Gholizadeh, S. (2016) 'A review of non-destructive testing methods of composite materials', Procedia Structural Integrity, 1, pp. 50–57. j.2016.

Yang, J. et al. (2019) 'Infrared Thermal Imaging-Based Crack Detection Using Deep Learning', IEEE Access, 7, pp. 182060./ACCESS.2019.

Shang, J. et al. (2007) 'Design of a climbing robot for inspecting aircraft wings and fuselage', Industrial Robot, 34(6), pp. 495–502.

Stamm, M. et al. (2021) 'In-plane heatwave thermography as digital inspection technique for fasteners in aircraft fuselage panels', Applied Sciences (Switzerland), 11(1), pp. 1–19. app11.

Cramer, K.E. and Winfree, W.P. (2006) 'The Application of Principal Component Analysis Using Fixed Eigenvectors to the Infrared Thermographic Inspection of the Space Shuttle Thermal Protection System', (July). doi:10.21611/qirt.2006.002.

Dwivedi, S.K., Vishwakarma, M. and Soni, P.A. (2018) 'Advances and Researches on Non Destructive Testing: A Review', Materials Today: Proceedings, 5(2), pp. 3690–3698. doi:10.1016/j.matpr.2017.11.620.

Eddazi, A. and Belattar, S. (2018) 'Nondestructive testing evaluation of aircraft fuselage corrosion by infrared thermography and finite element method', Proceedings - 2017 14th International Conference on Computer Graphics, Imaging and Visualization, CGiV 2017, pp. 56–61. doi:10.1109/CGiV.2017.13.

Faisal, N. et al. (2021) 'Defect Types', Springer Aerospace Technology, pp. 15–72. doi:10.1007/978-3-030-72192-3_3/FIGURES/57.

Gholizadeh, S. (2016) 'A review of non-destructive testing methods of composite materials', Procedia Structural Integrity, 1, pp. 50–57. doi:10.1016/j.prostr.2016.02.008.

Sause, M.G.R. (2021) Structural Health Monitoring Damage Detection Systems for Aerospace.

Shang, J. et al. (2007) 'Design of a climbing robot for inspecting aircraft wings and fuselage', Industrial Robot, 34(6), pp. 495–502. doi:10.1108/01439910710832093.

Srajbr, C., Bräutigam, K. and Dillenz, A. (2012) 'Crack Detection at Aluminum Fuselages by Induction Excited Thermography', (November 2012), pp. 3–8.

Stamm, M. et al. (2021) 'In-plane heatwave thermography as digital inspection technique for fasteners in aircraft fuselage panels', Applied Sciences (Switzerland), 11(1), pp. 1–19. doi:10.3390/app11010132.

Yang, J. et al. (2019) 'Infrared Thermal Imaging-Based Crack Detection Using Deep Learning', IEEE Access, 7, pp. 182060–182077. doi:10.1109/ACCESS.2019.2958264.

Author Biography

WPMY Thilakarathna completed the undergraduate academic programmneral Sir John Kotelawala Defence University (KDU), Sri Lanka and is waiting for e in Mechatronics Engineering from Gegraduation. Currently working as a Temporary Instructor at KDU. Her research interest includes mechanical designing, control systems and robotics.

AA Ziyard completed the undergraduate academic programme in the field of Mechatronics Engineering from KDU and waiting for the graduation,. Currently working as an Executive Autonomation Engineer at MAS Holdings, Sri Lanka. His research interest include machine designing , automobile and robotics.

ND Wijesinha completed the undergratuated academic programme in the field of Mechatronics Engineering from KDU and waiting for the graduation. Currently working as an Executive Autonomation Engineer at MAS Holdings, Sri Lanka. Her research interest include machine designing and automobile.

Col KVP Dhammika, Commanding Officer Cyber 12th Signal Corps Cyber Security Regiment of Sri Lanka Army and the Visiting Senior Lecturer at Faculty of Engineering, KDU. He obtained bachelor degree in Electronic Engineering from KDU and M.Phill in Electronic and Telecommunication Engineering from the University of Moratuwa Sri Lanka, MSc in Military Technology Degree from Pune University India.

GMSM Gaspe received the bachelors degree in Science and Technology specialized in Mechatronics from Uva Wellassa University of Sri Lanka in 2013. She has completed Masters in Applied Electronics at the University of Colombo in 2019. Currently, she is working as a lecturer at Faculty of Engineering, KDU. Her current research areas includes Intelligent Control Systems.